J. Chem. Sci. (2020) 132:130
https://doi.org/10.1007/s12039-020-01837-7

REGULAR ARTICLE

Structural investigation of barium zirconium titanate $Ba(Zr_{0.5}Ti_{0.5})O_3$ particles synthesized by high energy ball milling process

PELIN SÖZEN AKTAŞ
Department of Chemistry, Faculty of Arts and Sciences, Manisa Celal Bayar University, Şehit Prof. Dr. İlhan Varank Campus, Muradiye-Manisa 45140, Turkey
E-mail: pelin.sozen@cbu.edu.tr

MS received 22 June 2020; accepted 29 July 2020

Abstract. In this study, pure barium zirconium titanate $Ba(Zr_{0.5}Ti_{0.5})O_3$ (BZT) powders were successfully synthesized via the mechanochemical route using barium carbonate and titanium oxide as precursors. Structural properties of BZT are characterized by X-ray diffraction (XRD), Rietveld refinement, scanning electron microscope, energy dispersive X-ray spectrometry, thermogravimetric analysis, and FT-IR spectroscopy. It was observed that the ball milling operation has a significant influence on sintering temperature. Single-phase BZT was obtained under sintering conditions at 1350 °C. XRD and Rietveld refinement studies revealed that BZT composition has a cubic structure with a space group of *Pm-3m* (#221). As estimated by the Scherrer formula, the average crystallite size was determined as 79.2 nm for sintering temperature at 1350 °C.

Keywords. Barium zirconium titanate; High energy ball milling; X-ray diffraction; Rietveld.

1. Introduction

Since the discovery of the relaxor ferroelectrics in the 1950s, many kinds of research have been focused on the synthesis of perovskite materials to achieve their use in favorable capacitors and actuators.[1, 2] However, relaxor behavior was mainly obtained in lead-based and derived compositions. Unfortunately, because of the volatility and toxicity of the Pb-containing compounds, it has some severe drawbacks. Thus, the purpose of this study was to synthesize and characterize an environment-friendly Pb-free relaxor derived from BZT.

Many kinds of researches have been performed on $BaZr_xTi_{(1-x)}O_3$ (BZT) structures doped with zirconium in microwave devices and modern technology, due to their high dielectric constant, low dielectric loss and relatively high tunability.[3–5] Depending on the Zr content, BZT has been reported to have excellent dielectric properties when x is $x \leq 0.2$ and shows relaxor ferroelectric behavior at $x \geq 0.3$.[6, 7] At higher Zr concentration; a typical ferroelectric relaxation behavior have been observed.[8] Maiti *et al.*,[9] showed that the $BaZr_xTi_{1-x}O_3$ solid solution system had a polar cluster-like action at a higher $BaZrO_3$ concentration ($0.85 \geq x \geq 1.00$). In another study, the regular occurrence of relaxor behavior for the $0.50 \geq x \geq 0.80$ range was performed by substituting Ti^{4+} ions with Zr^{4+} in the $BaZrO_3$ matrix, which was very low dielectric constant.[10] However, studies on the synthesis and structural features of the $Ba(Zr_{0.5}Ti_{0.5})O_3$ in which it displays relaxor feature is limited.[2, 11]

The synthesis route for BZT powders is notable for determining the structural properties of these ceramics. However, under conventional solid-state route conditions, very high sintering temperatures (1500–1600 °C) is used for BZT ceramics. On the other hand, mechanochemical activation aims to produce solid-state reactions at lower temperatures than those used in conventional powder preparation methods. High energy ball milling is considered as an easy and inexpensive method for large-scale production of industrial materials.[12–14]

In previous studies related to the BZT system, the relaxor properties of ceramics obtained by sintering at high temperatures using the solid-state method were investigated in detail.[1, 2, 9, 10, 15] In the current study, the $Ba(Zr_{0.5}Ti_{0.5})O_3$ phase was prepared at 1350 °C with mechanochemical activation, and its structural features were tried to be elucidated. The reason for

*For correspondence

Published online: 23 September 2020

choosing $Ba(Zr_xTi_{1-x})O_3$ x = 0.5 is that it is located in the middle part of the relaxor regime. Also, the high energy ball milling method is essential in terms of contributing to future work.

In the present investigation, Ba $(Zr_{0.5}Ti_{0.5})O_3$ powders were synthesized by a high energy milling method. Structural properties were discussed with Rietveld refinement and solid-solid interdiffusion reaction observations in XRD.

2. Experimental

2.1 *Materials and method*

The $Ba(Zr_{0.5}Ti_{0.5})O_3$ powders were prepared by the high energy milling process. Barium carbonate ($BaCO_3$) (> 99.8 % purity, Alfa Aesar), zirconium oxide (ZrO_2) (99%, Fischer Scientific), titanium oxide (TiO_2) (99.5%, Sigma Aldrich) and isopropyl alcohol ($(CH_3)_2CHOH$, 99.5%, Sigma Aldrich) were used as starting materials.

FTIR spectra of the samples were recorded on Spectrum BX Perkin Elmer FT-IR System spectrometer using KBr pellets. Spectragryph Software for optical spectroscopy Version 1.2.13 was used to create multi-spectrum plots. Thermogravimetric analysis was performed for thermal analyses from 25 to 1200 °C at a heating rate of 10 °C/min on a thermal analyzer SII 7300 Perkin Elmer using flowing N_2 at 2.5 mL/min. Phase formation in the mechanically activated powders was characterized by using X-ray diffraction (XRD) on a PANalytical Empyrean diffractometer with Cu K_α radiation (λ = 1.5406Å). Match! Version 3 Crystal Impact was used for phase identification.[16] The Rietveld refinement program FULLPROOF analyzed the X-ray pattern of the corresponding compound.[17] Scanning electron microscopy (SEM) was used to analyze the morphology of the $Ba(Zr_{0.5}Ti_{0.5})O_3$ structure. SEM images were taken by a Zeiss Gemini 500 microscope. The average particle diameters were measured from each SEM image. Energy-dispersive X-ray spectroscopy (EDS) was used to ascertain the chemical composition of the material. EDS studies were performed by using a ZEISS (Gemini 500) SEM operating at an accelerating voltage of 15 kV.

2.2 *Synthesis of BZT particles*

The powders of $BaCO_3$ (10 g), ZrO_2 (3.14 g) and TiO_2 (2.019 g) were weighed in proportion to the stoichiometric ratio and mixed and stirred in isopropyl alcohol (IPA) for 30 min. The mixture of powders dried at 100 °C for 2 h in a vacuum oven. The dried powder was then high energy milled using a Retsch PM100 type planetary ball milling system at room temperature for 4 h. The milling speed was set at 300 rpm and was stopped for 5 min for milling every 25 min to cool the system. Carbide balls with a diameter of 10 mm were operated in the milling procedure. The powder mass/ball mass ratio was used as 1:5.19. In the grinding process, a 250 mL tungsten carbide jar and ten balls (78.07 g) were operated. The milled powders were heat-treated at 1000 °C, 1050 °C, 1200 °C, 1300 °C, and 1350 °C for 4 h with a heating rate of 10 °C/min and then slowly cooled at room temperature.

3. Results and Discussion

3.1 *Phase formation from X-ray diffraction*

The XRD results showed comprehensible diffraction peaks. The major peak was identified to the cubic phase indicating that of $Ba(Zr_{0.5}Ti_{0.5})O_3$ (BZT) powder was synthesized by high energy ball milling method. The XRD patterns for phase formation at different temperatures are given in Figure 1. As clearly observed here, the BZT structure started to form at 1300 °C. XRD results confirmed that milled powder crystallizes into single-phase formation, and an intermediate product formation was also not observed. At 1000 °C, $BaTiO_3$ (BT) and $BaZrO_3$ (BZ) phases occurred separately and approximately equally. At the same temperature, a trace amount of $BaCO_3$ is also present in the reaction medium. It was disappeared entirely at 1200 °C, and the BZT peak started

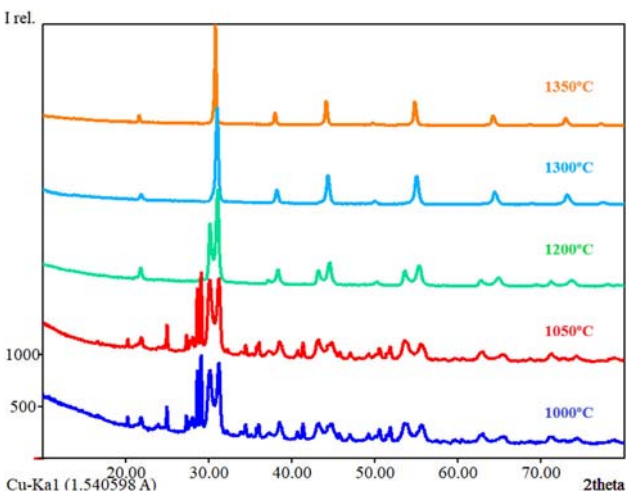

Figure 1. XRD patterns of BZT powders sintered for 4 hours at 1000 °C, 1050 °C, 1200 °C, 1300 °C, and 1350 °C.

to rise. Figure 2 illustrates the phase formation of XRD patterns between 25 and 35° 2θ values. In XRD patterns at 1300 °C and 1350 °C, the corresponding (110) diffraction peaks shift from 31.16° to 30.84°. It is important to note here that diffraction peaks move to lower angles as the Zr content (BZ) decreases. This observation is indicating that BZ has thoroughly diffused into the BT lattice. Considering the ionic radii of Ti^{4+} (0.605 Å) and Zr^{4+} (0.72 Å), it can be mentioned that BZ expands the BT lattice. When XRD patterns are considered, it is recognized that BT and BZ are formed at 1200 °C, and BZT structure is formed over 1200 °C. BZT was achieved by the interdiffusion of the reaction BT and BZ. Bera *et al.*,[6] reported similar observations.

3.2 *Rietveld refinement analysis*

The refinement of the crystal structure was performed by the Rietveld method. Rietveld refinement results of XRD profiles are given in Figure 3. All the peaks are indexed for the cubic phase formation, and lattice powders indicate the formation of the cubic phase, which belongs to space group Pm–3m (#221). The lattice parameters obtained from Rietveld refinement were a = 4.0980 Å, V = 68.821 $Å^3$, and calculated density of 6.139 g/cm^3. The parameters of refinement are R_F = 3.37 and χ^2 = 5.18. The refinement results obtained from in this study positively confirmed that the BZT phase maintains the cubic crystal system, and this is in an excellent agreement with those reported in the literature for $Ba(Zr_{0.5}Ti_{0.5})O_3$ structure.[2,11,15] The average crystallite sizes, which are estimated by the Scherrer formula (which was automatically calculated from Match! Programme), were 37.02 nm and 79.27 nm for sintering temperatures of 1300 °C and 1350 °C, respectively.

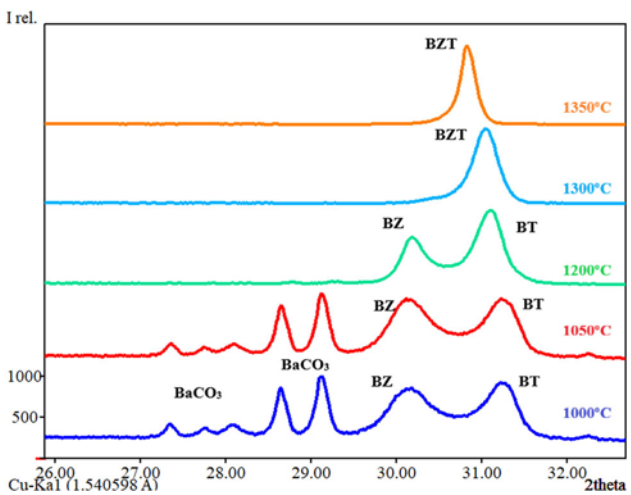

Figure 2. Detailed representation of the 25–35° 2θ range of XRD patterns. (BT: $BaTiO_3$, BZ: $BaZrO_3$ and BZT: $Ba(Zr_{0.5}Ti_{0.5})O_3$)

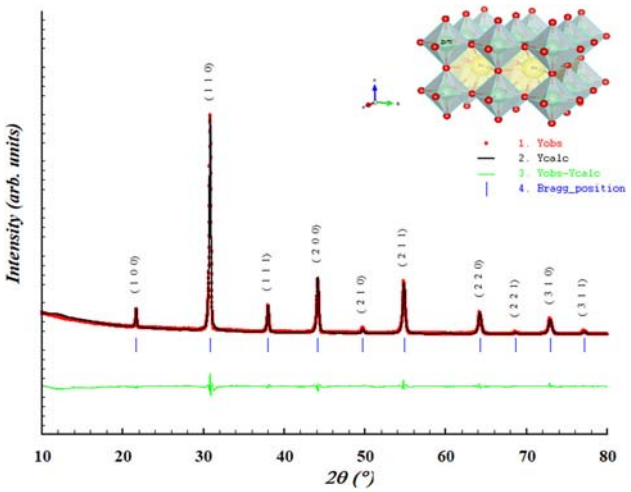

Figure 3. Rietveld refinement of BZT sintered at 1350 °C for 4 h. Experimental (1) and calculated (2) diffraction patterns of BZT material after Rietveld refinement. Difference (3), Bragg Positions (4). The inset shows the crystal structure of $Ba(Zr_{0.5}Ti_{0.5})O_3$. Barium atom has 12-fold coordination and in the center of the cell. Zr/Ti atom at the corner of the cell.

A summary of the refinement details for the $Ba(Zr_{0.5}Ti_{0.5})O_3$ powder is interpreted in Table 1. As clearly seen here, the table includes lattice and refinement parameters. R factors show a reliable structural model. In the Rietveld refinement, the Pseudo-Voigt function was used with standard Debye Scherrer geometry to describe the peak shape. A reasonably exact fit between the predicted and measured diffraction patterns were observed and verified the accuracy of the refinement.

Table 1. Refined structural parameters and reliability factor values for $Ba(Zr_{0.5}Ti_{0.5})O_3$

Formula	$Ba(Zr_{0.5}Ti_{0.5})O_3$
Formula weight	240.716 g/mol
Temperature (*K*)	298
λ (Å)	1.54060
Crystal system	cubic
space group	*Pm–3m* (#221)
Unit cell dimensions	a=4.098Å,
V ($Å^3$)	68.821
Calc. Density (g/cm^3)	6.139
2θ range	10.0078–79.9922
(step)(°)	0.0131
$\chi 2$	5.18
R_F, R_{Bragg} (%)	3.37, 4.26
R_p, R_{wp}, R_{exp} (%)	3.56, 4.79, 2.11

3.3 *TGA analysis*

The results of the thermal analyses are of considerable importance to understand the decomposition mechanism of the precursors and, thereby, the ceramic oxide's formation with preferred properties. Figure 4 shows the DTG, DTA, and TG curves obtained for the milling samples. In the TGA of milled powder, the first region from 25 °C to 600 °C corresponds to the removal of moisture and volatiles (solvent, IPA) with a total loss of about 1.73%. The TGA graph also shows a single step of degradation from 600 °C to 974 °C with total loss % 14.92, which indicates the evolution of CO_2. Similar observations have been reported for $Ba(Zr_{0.6}Ti_{0.4})O_3$ composition.[6] The BT and BZ samples left at $\geq$ 1000 °C stable and is about 83% of the original sample weight. As can be detected in the XRD patterns between 1000–1050 °C, no intermediate products like BaO or other phases formation are observed besides the BT, BZ, and minor amount of $BaCO_3$ components. In the DTA curve, a sharp endothermic peak at 919 °C indicates the significant phase transformation of $BaCO_3$. According to Seetharaman *et al.,* $BaCO_3$ shows two-phase conversions, one at 806 °C (corresponding to an orthorhombic to-hexagonal transformation) and another at 968 °C (hexagonal $BaCO_3$ to cubic form).[18] The two endothermic peaks in the DTA curve at 830 and 916 °C obtained in the present work match to these two-phase transformations. As a result, BT and BZ are formed according to the direct reaction of:

$$BaCO_{3(solid)} + TiO_{2(solid)} = BaTiO_{3(solid)} + CO_{2(g)}$$

$$BaCO_{3(solid)} + ZrO_{2(solid)} = BaZrO_{3(solid)} + CO_{2(g)}$$

Furthermore, in the second step, interdiffusion between $BaTiO_3$ and $BaZrO_3$ of giving resulted in $Ba(Zr_{0.5}Ti_{0.5})O_3$ structure.

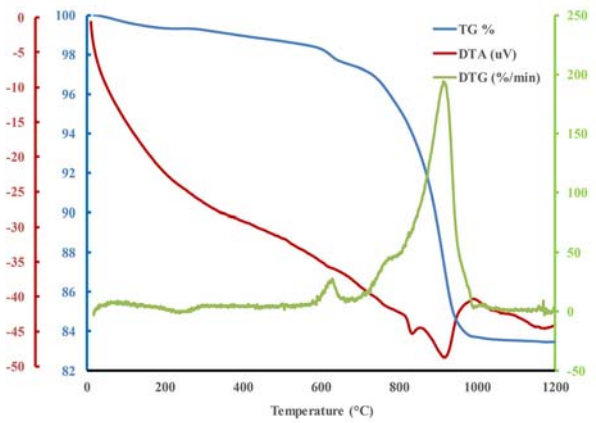

Figure 4. TGA, DTA, and DTG curves for the ball-milled powders of starting precursors.

3.4 *FT-IR analysis*

The phase identification of barium zirconium titanate $Ba(Zr_{0.5}Ti_{0.5})O_3$ powder synthesized by high energy ball milling technique was further investigated by FT-IR analysis. Figures 5 and 6 shows the FT-IR spectra of milled powder at room temperature and heat-treated at different temperatures. The figure shows typical IR absorption bands of isopropyl alcohol in the ranges of 2800–3000 cm^{-1} and 3000–3400 cm^{-1} and, these bands are assigned to be C–H stretch of methyl groups and O–H stretching vibrations respectively.[19] In the spectrum of milled powder characteristic peaks at 1751 cm^{-1} (stretching vibration of C=O), 1433 cm^{-1} (asymmetric stretching vibrations of C–O), 859 and 693 cm^{-1} (O–C–O bending vibrations) belong to $BaCO_3$.[20] With increasing sintering temperature, the peaks at 1750, 1434 and 858 cm^{-1} gradually decreased and disappeared entirely at 1200 °C. Two peaks began the form at 550 cm^{-1} in the BZT sample, which sintered at 1300 °C. The absorption bands in the range of 400–600 cm^{-1} are often attributed to the formation of Zr-O and Ti-O

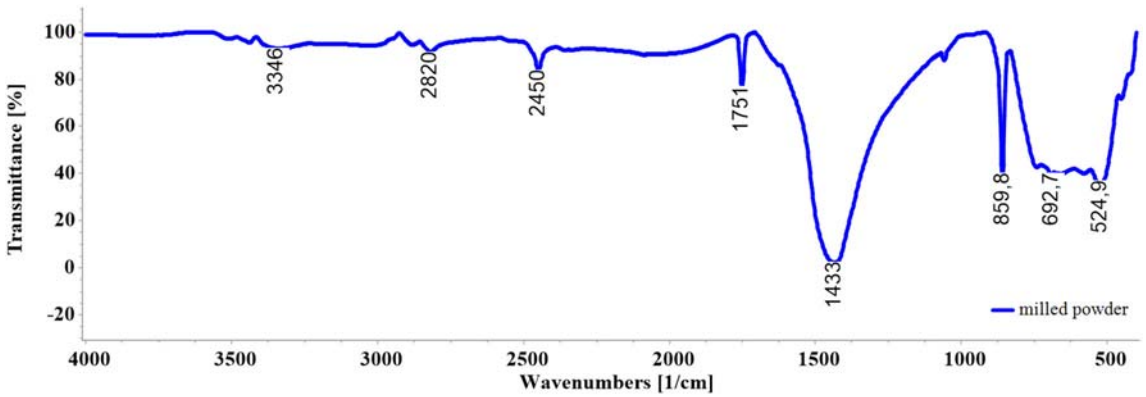

Figure 5. Detailed FT-IR spectrum of milled BZT powders at room temperature.

stretching vibrations.[7] The peaks at 578 cm^{-1} and 527 cm^{-1} can be assigned to vibrations of TiO_6 and ZrO_6 octahedra. The results of the FT-IR spectra are compatible with XRD and TGA-DTA analysis, confirming that the formation temperature of BZT powder is over 1200 °C.

3.5 *SEM analysis*

The Sem micrographs of reaction intermediates of BZT particles sintered at 1200 °C are represented in Figure 7(a–d). At 1200 °C, a mixture of BT, BZ, and BZT was started form, and the grains were generally rounded shape and 50–200 nm in size. The morphology of the synthesized BZT powders at 1300 °C and 1350 °C is represented in Figure 8. It was observed here that, the particles agglomerated (Figure 8b and e, respectively) and irregularly distributed in a partially uniform size. At these temperatures (1300 °C and 1350 °C), the average grain size is determined between ∼300 and ∼ 350 nm with polygonal-shape (Figure 8c and f). Figure 8c includes lamellar as

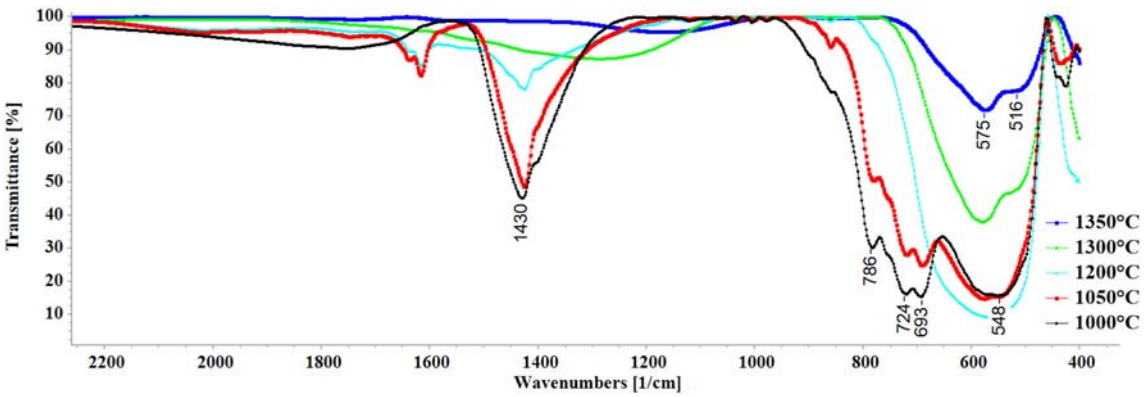

Figure 6. FT-IR spectra of BZT powders at different temperatures.

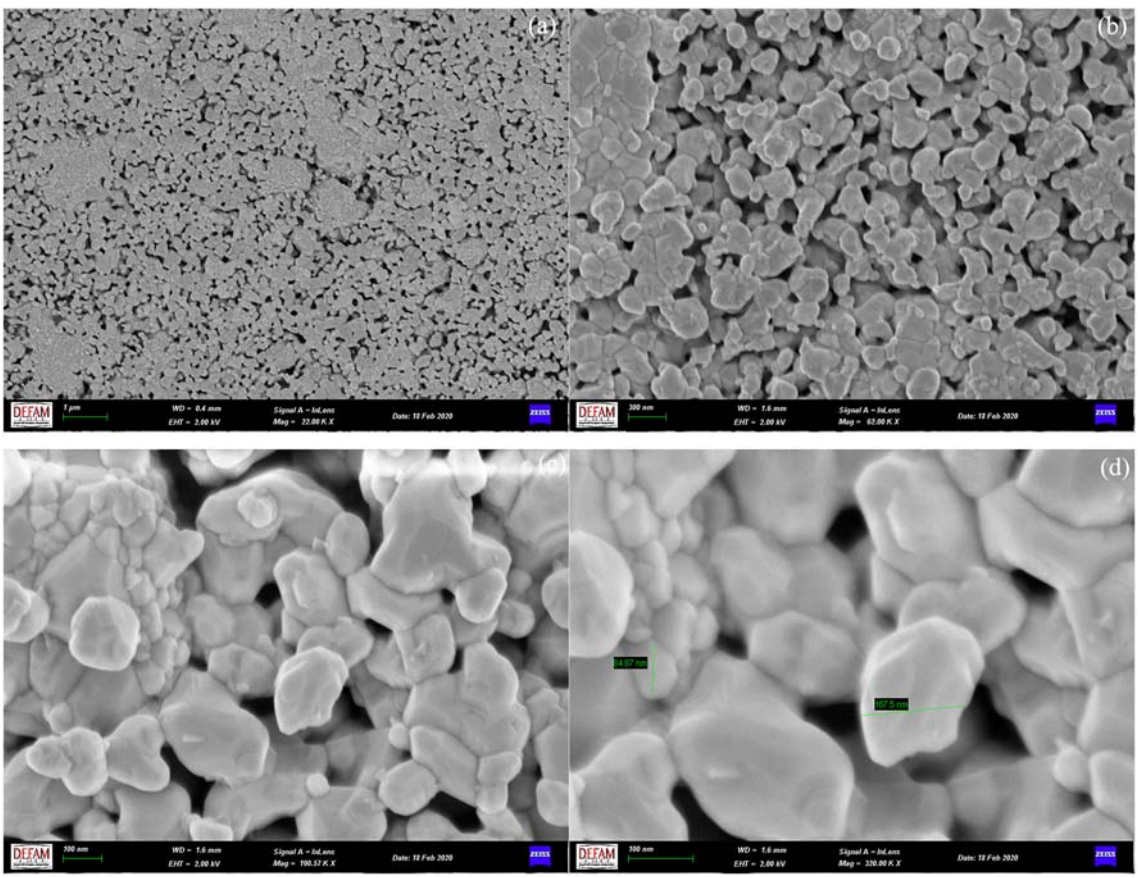

Figure 7. Sem micrographs of BZT particles sintered 1200 °C for 4 h.

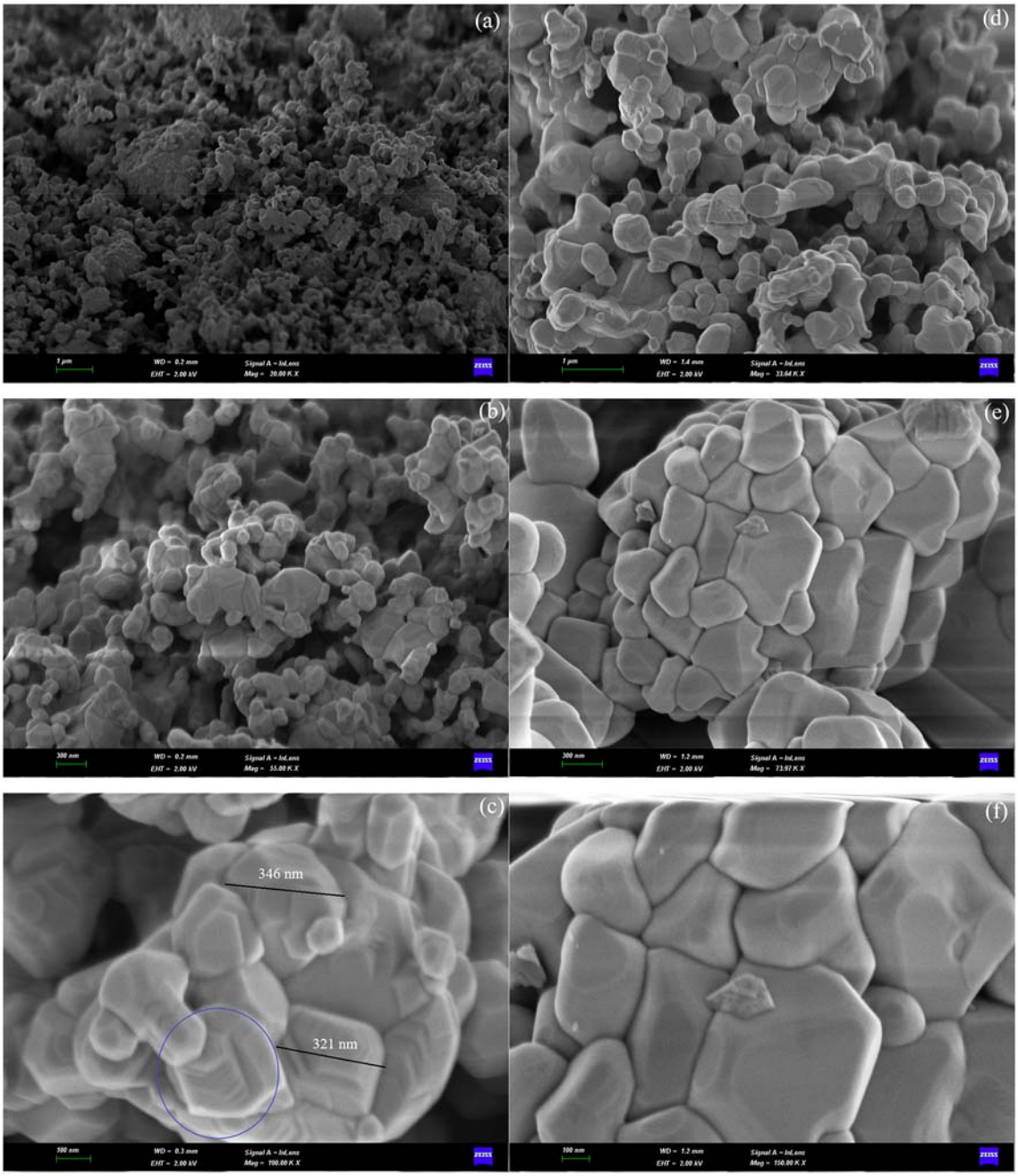

Figure 8. Sem micrographs of BZT particles sintered at 1300 °C (**a**)–(**c**) and 1350 °C (**d**)–(**f**).

indicated with blue frame character.[21] It is seen in Sem micrographs that the grain size in the sample increases with increasing temperature.[22] Here, it can be stated that densification does not occur; coarsening in the atomic process is dominant, therefore the grain size increases.[23,24] EDS analysis of BZT particles sintered at 1350 °C for 4 h is given in Figure 9 and confirmed the accuracy of elemental composition. The compositions of synthesized BZT were found to have a very close agreement with the experimentally calculated compositions of material.

Considering XRD results at 1200 °C, 1300 °C and 1350 °C, BT, and BZ structures formed separately, and Zr^{4+} ions diffuse into BT lattices. Similar observations were reported by Bera *et al.*[6] As noticed in XRD studies (Figure 2), the quantity of BT formed in the range of 1000–1200 °C is more than BZ. This difference in amount can be considered to be due to the different activation energies of these compounds (34.3 kcal/mol for BT, and 48.4 kcal/mol for BZ).[25] It can be assumed that the BZT formation occurs in two steps, BT and BZ occur separately in the first step, and

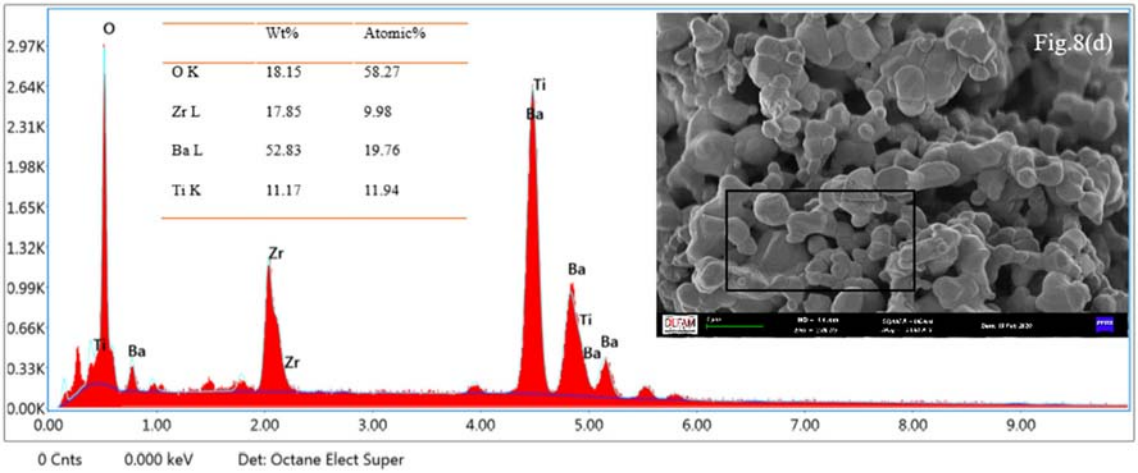

Figure 9. EDS spectra of BZT sintered at 1350 °C for 4 h.

BZ diffuses to BT in the second step. In the TGA curve (Figure 4), it is detected that the phase formation where the curve remains constant over 1000 °C occurs.

In previous studies, BZT structure has been synthesized as solid-state, chemical synthesis from solution, and sol-gel method.[2,26,27] In the solid-state process, it is unadvantageous to perform at high temperatures of 1500–1600 °C and to use non-economical starting materials like barium hydroxide, zirconium isopropoxide, tetrabutyl titanate in chemical routes.

In this study, the BZT structure was achieved at 1350 °C by using a high energy ball milling method. The reaction was followed between 1000–1350 °C by XRD, and no intermediate product was observed. The structure was also supported by Rietveld analysis. A detailed investigation of the structure will contribute to the electronic applications of lead-free relaxor material BZT.

4. Conclusions

In this presented work, pure $Ba(Zr_{0.5}Ti_{0.5})O_3$ (BZT) was successfully synthesized via the mechanochemical method, and its microstructure was evaluated. Phase formation was followed with XRD, which were monitored at 1050–1350 °C temperature ranges. It was found that the ball milling process has a significant influence on sintering temperature. Compared with the solid-state method, at a low sintering temperature of 1350 °C was obtained as pure material. It is more advantageous than the repeated grinding and heating process in the solid-state technique, although sub-micron grain size is achieved by this method. The SEM micrographs of powder showed that the BZT particles are polygonal in shape, and the average grain size is observed about 300–350 nm. The structure of BZT, which is an environmentally friendly lead-free relaxor obtained at a lower temperature, has been tried to be elucidated in detail. The study will contribute to future research on the relaxor features of BZT.

Acknowledgements

The author thanks the financial support of the Scientific Research Project Office of Manisa Celal Bayar University (Project No: 2019-056).

References

1. Filipič C, Kutnjak Z, Pirc R, Canu G and Petzelt J 2016 $BaZr_{0.5}Ti_{0.5}$ O_3: Lead-free relaxor ferroelectric or dipolar glass *Phys. Rev. B* **93** 1
2. Maiti T, Guo R and Bhalla A S 2011 Evaluation of experimental resume of $BaZr_xTi_{1-x}O_3$ with perspective to ferroelectric relaxor family: An overview *Ferroelectrics* **425** 4
3. Binhayeeniyi N, Sukwisute P, Safitree N and Muensit N 2020 Energy Conversion Capacity of Barium Zirconate Titanate *Materials (Basel)*. **13** 1
4. Bhargavi G N, Khare A, Badapanda T, Anwar M S and Brahme N 2018 Analysis of temperature and frequency dependent dielectric properties, dynamic hysteresis loop and thermal energy conversion in $BaZr_{0.05}Ti_{0.95}O_3$ ceramic *J. Mater. Sci. Mater. Electron.* **29** 11439
5. Dong L, Stone D S and Lakes R S 2012 Enhanced dielectric and piezoelectric properties of $xBaZrO_3$-(1-x)$BaTiO_3$ ceramics *J. Appl. Phys.* **111** 084107
6. Bera J and Rout S K 2005 On the formation mechanism of $BaTiO_3$-$BaZrO_3$ solid solution through solid-oxide reaction *Mater. Lett.* **59** 135
7. Seeharaj P, Boonchom B, Charoonsuk P, Kim-Lohsoontorn P and Vittayakorn N 2013 Barium zirconate titanate nanoparticles synthesized by the sonochemical method *Ceram. Int.* **39** 559

8. Ma Y B, Molin C, Shvartsman V V, Gebhardt S, Lupascu D C, Albe K and Xu B X 2017 State transition and electrocaloric effect of BaZrxTi1-xO_3: Simulation and experiment *J. Appl. Phys*. **121** 024103
9. Maiti T, Guo R and Bhalla A S 2008 Structure-property phase diagram of $BaZr_xTi_{1-x}O_3$ system *J. Am. Ceram. Soc*. **91** 1769
10. Maiti T, Guo R, Bhalla and A S 2006 Electric field dependent dielectric properties and high tunability of $BaZr_xTi_{1-x}O_3$ relaxor ferroelectrics *Appl. Phys. Lett*. **89** 2012
11. Chauhan R and Srivastava R C 2015 Dielectric study of $BaZr_{0.5}Ti_{0.5}O_3$ ferroelectric relaxor ceramic *Int. J. Electron. Commun. Eng*. **4** 1
12. Kong L B, Ma J, Huang H, Zhang R F and Que W X 2002 Barium titanate derived from mechanochemically activated powders *J. Alloys Compd*. **337** 226
13. Gusev A I and Kurlov A S 2008 Production of nanocrystalline powders by high-energy ball milling: Model and experiment *Nanotechnology* **19** 265302
14. Nath A K, Jiten C and Singh K C 2010 Influence of ball milling parameters on the particle size of barium titanate nanocrystalline powders *Phys. B Condens. Matter* **405** 430
15. Maiti T, Guo R and Bhalla A S 2006 The evolution of relaxor behavior in Ti^{4+} doped $BaZrO_3$ ceramics *J. Appl. Phys*. **100** 114119
16. Match! - Phase Identification from Powder Diffraction, Crystal Impact - Dr. H. Putz & Dr. K. Brandenburg GbR, Kreuzherrenstr. 102, 53227 Bonn, Germany. http://www.crystalimpact.com/match.
17. Rodríguez-Carvajal J 1993 Recent advances in magnetic structure determination by neutron powder diffraction *Phys. B: Phys. Condens. Matter* **192** 55
18. Arvanitidis I, Sichen D and Seetharaman S 1996 A study of the thermal decomposition of $BaCO_3$ *Metall. Mater. Trans. B Process Metall. Mater. Process. Sci.* **27** 409
19. Coates J 2004 Interpretation of Infrared Spectra, A Practical Approach *Encycl. Anal. Chem.* 1
20. Sabet M, Salavati-Niasari M and Fard Z A 2016 Synthesis and characterization of Barium carbonate nanostructures via simple hydrothermal method *Synth. React. Inorganic Met. Nano-Metal Chem.* **46** 317
21. Cai W, Fu C, Gao J and Chen H 2009 Effects of grain size on domain structure and ferroelectric properties of barium zirconate titanate ceramics *J. Alloys Compd.* **480** 870
22. Jha P A and Jha A K 2012 Influence of processing conditions on the grain growth and electrical properties of barium zirconate titanate ferroelectric ceramics *J. Alloys Compd.* **513** 580
23. Barsoum M W 2002 *Fundamentals of Ceramics* B Cantor and M J Goringe (Eds.) (Bristol and Philadelphia: IOP Publishing Ltd.) p.304
24. Kingery W D, Bowen H K and Uhlmann D R 1976 *Introduction to Ceramics* E Burke, Chalmers B and J A Krumhasl (Eds.) (Newyork: John Wiley and Sons) p.452
25. Mikhailov M M, Neshchimenko V V, Utebekov T A and Yuriev S A 2015 Features high-temperature synthesis of barium zirconium titanate powder by using zirconium dioxide nanopowders *J. Alloys Compd*. **652** 364
26. Veith M, Mathur S, Lecerf N, Huch V, Decker T, Beck H P, Eiser W and Haberkorn R 2000 Sol-gel synthesis of nano-scaled $BaTiO_3$, $BaZrO_3$ and $BaTi_{0.5}Zr_{0.5}O_3$ oxides via single-source alkoxide precursors and semi-alkoxide routes *J. Sol-Gel Sci. Technol*. **17** 145
27. Qi J Q, Wang Y, Chen W P, Li L T and Chan H L W 2006 Perovskite barium zirconate titanate nanoparticles directly synthesized from solutions *J. Nanoparticle Res*. **8** 959